Stochastic multiresonance and correlation-time-controlled stability for a harmonic oscillator with fluctuating frequency

Romi Mankin, Katrin Laas, and Tõnu Laas*
Institute of Mathematics and Natural Sciences, Tallinn University, 25 Narva Road, 10120 Tallinn, Estonia

Eerik Reiter
Institute of Physics, Tallinn University of Technology, 5 Ehitajate Tee, 19086 Tallinn, Estonia
(Received 6 July 2008; published 17 September 2008)

The long-time behavior of the first two moments and the correlation function for the output signal of a harmonic oscillator with fluctuating frequency subjected to an external periodic force and an additive thermal noise is considered analytically. The colored fluctuations of the oscillator frequency are modeled as a three-level Markovian noise. Using the Shapiro-Loginov formula, the exact expressions of several stochastic resonance (SR) characteristics such as the spectral amplification, the variance of the output signal, the signal-to-noise ratio, and the SR gain have been calculated. The nonmonotonic dependence of the SR characteristics versus the noise parameters as well as versus the input signal frequency and also the conditions for the appearance of energetic instability are analyzed. In particular, the multiresonancelike behavior of the variance and the signal-to-noise ratio as functions of the noise correlation time are observed and the connection between the occurrence of energetic instability and the phenomenon of stochastic multiresonance is established. Some unexpected effects such as the hypersensitive response of the spectral amplification to small variations of the noise amplitude encountered in the case of a large flatness of the colored noise are also discussed.

DOI: 10.1103/PhysRevE.78.031120 PACS number(s): 05.40.−a, 02.50.−r

I. INTRODUCTION

The past decades have witnessed an increasing interest in noise-induced phenomena in nonequilibrium systems. Stochastic ratchets [1], noise-induced spatial patterns [2], hypersensitive transport [3], stochastic resonance [4], noise-induced multistability, and discontinuous transitions [5], are a few examples in this field. One of the objects of special attention in this context is the noise-driven harmonic oscillator. The harmonic oscillator is the simplest toy model for different phenomena in nature and as such it is the typical theoretician's paradigm for various fundamental conceptions [6]. The problem of noise-driven dynamics of a Brownian harmonic oscillator was earlier formulated and solved by Chandrasekhar [7], using the Langevin and Fokker-Planck equations. Since then the Chandrasekhar model and its many variants have been reappearing in literature. For example, the study of a harmonic oscillator with random frequency is a subject that has been extensively investigated in different fields including physics [8,9], biology [10], chemistry [11], etc. In most of the previous analysis the influence of white noise is considered. However, more realistic models of physical systems, such as, e.g., the dynamics of a dye laser and the transport of proteins in cells that works in the presence of thermal noise and colored noise of biological origin, require considering a system simultaneously driven by white noise and colored noise. It is shown that the influence of colored noise on the oscillator frequency may lead to different resonant phenomena. First, it may cause energetic instability, which manifests itself in an unlimited increase of the second-order moments of the output with time, while the mean value of the oscillator displacement remains finite [8,12,13]. This phenomenon is a stochastic counterpart of classical parametric resonance [8,14]. Second, if the oscillator is subjected to an external periodic force and the fluctuations of the oscillator frequency are colored, the behavior of the amplitude of the first moment shows a nonmonotonic dependence on noise parameters, i.e., stochastic resonance (SR) [15,16]. To avoid misunderstandings, let us mention that we use the term SR in the wide sense, meaning the nonmonotonic behavior of the output signal or some function of it (moments, autocorrelation functions, signal-to-noise ratio) in response to the noise parameters [15,17]. Third, in some cases a bona fide resonance appears, where the moments and the signal-to-noise ratio (SNR) show a nonmonotonic dependence on the frequency of external forcing [16,18].

Surprisingly, the existence of SR in the case of a harmonic oscillator has never been linked to the potential consequences of the energetic instability. Moreover, although the two most common quantifiers for SR are the average output amplitude, or the spectral amplification (SPA) and the signal-to-noise ratio [4], it seems that the analysis of the behavior of SNR for an underdamped harmonic oscillator with colored noise excitations is still missing in literature.

Thus motivated, we consider a model similar to the one presented in [15], except for some details of the noises, i.e., a harmonic oscillator with fluctuating frequency subjected to an external sinusoidal force and an additive thermal noise. The fluctuations of the frequency are modeled as a three-level Markovian noise (trichotomous noise) [19]. Note that in the model presented in [15] the thermal noise is absent and the colored fluctuations of the frequency are assumed to be a dichotomous noise. Although both dichotomous and trichotomous noises may be useful in modeling natural colored fluc-

*tony@tlu.ee

tuations, the latter is more flexible, including all cases of dichotomous noise. Furthermore, it is remarkable that for trichotomous noises the flatness parameter κ, in contrast to the Gaussian colored noise, $\kappa=3$, and symmetric dichotomous noise, $\kappa=1$, can be anything from 1 to ∞. This extra degree of freedom can prove useful in modeling actual fluctuations.

The main contribution of this paper is as follows. We provide exact formulas for the analytic treatment of the dependence of SR characteristics (SNR, SR gain, variance of the output signal, and spectral amplification) on various system parameters: viz. temperature, correlation time, flatness, noise amplitude, and frequency of the input signal. Furthermore, we establish the sufficient and necessary conditions for the occurrence of energetic instability and analyze the behavior of the instability region in the system parameter space. In some regions of the system parameters, variations of the noise correlation time can cause transitions between the stable and unstable energetic states of the oscillator. The corresponding transitions are found to be reentrant, e.g., the instability appears above a critical value of the noise correlation time, but disappears again at a still higher value. On the basis of exact expressions for SR characteristics we find a number of cooperation effects arising as a consequence of an interplay between multiplicative trichotomous noise, thermal noise, and a deterministic force, e.g., (i) a hypersensitive response of SPA to variations of noise amplitude; (ii) sharp suppressions of SR gain at some values of the input signal frequency by a high noise flatness; (iii) a multiresonance behavior versus the correlation time of the output variance and SNR associated with the critical characteristics of stochastic parametric resonance.

The structure of the paper is as follows. In Sec. II we present the model investigated. A description of the output SR quantifiers is given and exact formulas are found for the analysis of the long-time behavior of SPA, variance, SNR, and SR gain. In Sec. III we analyze the conditions of energetic instability and the dependence of the SR characteristics on system parameters. Section IV contains some brief concluding remarks. Some formulas are delegated to the Appendix.

II. MODEL AND THE EXACT MOMENTS

A. Model

As an archetypical model for an oscillatory system strongly coupled with a noisy environment, we consider the stochastically perturbed harmonic oscillator with a random frequency

$$\ddot{X} + \gamma\dot{X} + [\omega^2 + Z(t)]X = A_0 \sin \Omega t + \xi(t), \tag{1}$$

where $\dot{X} \equiv dX/dt$, $X(t)$ is the oscillator displacement, γ is a damping parameter, the driving force $\xi(t)$ is a Gaussian white noise with a zero mean and with the δ-correlated correlation function given by

$$\langle \xi(t)\xi(t')\rangle = 2D\delta(t-t'). \tag{2}$$

Fluctuations of the frequency ω^2 are expressed by a Markovian trichotomous noise $Z(t)$, which consists of jumps between three values: $z_1=a$, $z_2=0$, $z_3=-a$, $a>0$ [19]. The jumps follow, in time, the pattern of a Poisson process, the values occurring with the stationary probabilities $p_s(a)=p_s(-a)=q$ and $p_s(0)=1-2q$, where $0<q<1/2$. In a stationary state the fluctuation process $Z(t)$ satisfies

$$\langle Z(t)\rangle = 0, \quad \langle Z(t+\tau)Z(t)\rangle = 2qa^2e^{-\nu\tau}, \tag{3}$$

where the switching rate ν is the reciprocal of the noise correlation time $\tau_c=1/\nu$, i.e., $Z(t)$ is a symmetric zero-mean exponentially correlated noise. The trichotomous process is a particular case of a kangaroo process [20] with the flatness parameter

$$\kappa = \frac{\langle Z^4(t)\rangle}{\langle Z^2(t)\rangle^2} = \frac{1}{2q}. \tag{4}$$

In this work, we will restrict ourselves to the case where for all states of the trichotomous noise the frequency of the oscillator is positive, i.e.,

$$a < \omega^2. \tag{5}$$

To find the first and second moments of X we use the well-known Shapiro-Loginov procedure [21], which for an exponentially correlated noise $Z(t)$ yields

$$\frac{d}{dt}\langle Zm\rangle = \left\langle Z\frac{dm}{dt}\right\rangle - \nu\langle Zm\rangle, \tag{6}$$

where m is some function of the noise, $m=m(Z)$.

B. First moments

From Eqs. (1) and (6), we thus obtain an exact, linear system of six first-order differential equations (A1) for six variables, $M_{1,1}\equiv\langle X\rangle$, $M_{1,2}\equiv\langle\dot{X}\rangle$, $M_{1,3}\equiv\langle ZX\rangle$, $M_{1,4}\equiv\langle Z\dot{X}\rangle$, $M_{1,5}\equiv\langle Z^2X\rangle$, $M_{1,6}\equiv\langle Z^2\dot{X}\rangle$. The solution of equations (A1) can be represented in the form

$$M_{1,i} = A_{2i-1}\sin(\Omega t) + A_{2i}\cos(\Omega t) + \sum_{j=1}^{6} C_j L_{i,j} e^{\rho_j t}, \tag{7}$$

where the coefficients L_{ij}, $i,j=1,\ldots,6$, are given by Eqs. (A2) and C_j are constants of integration determined by initial conditions, and $\{\rho_j, j=1,\ldots,6\}$ is the set of roots of the algebraic equation

$$[\omega^2 + \rho(\rho+\gamma)][\omega^2 + (\rho+\nu)(\rho+\nu+\gamma)]^2 - a^2[\omega^2 + \rho(\rho+\gamma) + 2q\nu(2\rho+\gamma+\nu)] = 0. \tag{8}$$

The coefficients A_k, $k=1,\ldots,12$, are given by Eqs. (A3) with (A4) in the Appendix. Note that the moments $M_{1,j}$ are independent of the thermal noise $\xi(t)$. One can check the stability of the solution (7), which means that the solution of Eq. (8) cannot have roots with a positive real part. According to the Routh-Hurwitz theorem [22] this requirement is met by the sixth-order polynomial in ρ in Eq. (8) for all values of the parameters, if the inequality (5) holds. Thus in the long time limit, $t\to\infty$, the moments $M_{1,j}$ are given by

$$M_{1,i|t\to\infty} = M_{1,i}^{(as)} = A_{2i-1}\sin(\Omega t) + A_{2i}\cos(\Omega t), \quad i = 1, \ldots, 6. \tag{9}$$

Particularly, the first moment $M_{1,1}^{(as)} = \langle X\rangle_{as}$ reads as

$$\langle X\rangle_{as} = A\sin(\Omega t + \varphi), \tag{10}$$

where

$$A^2 = A_1^2 + A_2^2 = \frac{A_0^2[f_1^2 + (f_2 + 2qa^2)^2]}{f_3^2 + f_4^2}, \tag{11}$$

$$\tan\varphi = \frac{f_1 f_3 - f_4(f_2 + 2qa^2)}{f_1 f_4 + f_3(f_2 + 2qa^2)}, \tag{12}$$

and the quantities f_i $(i=1,\ldots,4)$ are determined by Eqs. (A4).

C. Second moments

Here we will evaluate the long-time behavior of the moments, $M_{2,1} \equiv \langle X^2\rangle$, $M_{2,2} \equiv \langle X\dot{X}\rangle$, $M_{2,3} \equiv \langle ZX^2\rangle$, $M_{2,4} \equiv \langle ZX\dot{X}\rangle$, $M_{2,5} \equiv \langle Z^2X^2\rangle$, $M_{2,6} \equiv \langle Z^2X\dot{X}\rangle$, $M_{2,7} \equiv \langle \dot{X}^2\rangle$, $M_{2,8} \equiv \langle Z\dot{X}^2\rangle$, $M_{2,9} \equiv \langle Z^2\dot{X}^2\rangle$.

Starting from Eqs. (A5) and (9), we obtain that in the limit $t\to\infty$ the moments $M_{2,i}^{(as)} = M_{2,i|t\to\infty}$ are given by

$$M_{2,i}^{(as)} = N_i + J_{2i-1}\sin(2\Omega t) + J_{2i}\cos(2\Omega t), \quad i = 1, \ldots, 9, \tag{13}$$

where the constants N_i and J_k are determined with sets of algebraic linear equations. Note that the result (13) is correct only under the implicit assumption of energetic stability, i.e., the roots of the characteristic polynomial equation of the nine first-order differential equations determining the moments $M_{2,i}$, $i=1,\ldots,9$, cannot have positive real parts. This characteristic polynomial equation reads as

$$\begin{aligned}&(\rho+\gamma+\nu)((\rho+\gamma)(\rho+\gamma+\nu)[4\omega^2 + \rho(\rho+2\gamma)]\\ &\quad\times\{[4\omega^2 + (\rho+\nu)(\rho+\nu+2\gamma)]^2 - 16a^2\}\\ &\quad - 8qa^2\nu\{\nu[4\omega^2 + \rho(\rho+2\gamma)] + (2\rho+2\gamma+\nu)^3\}) = 0.\end{aligned} \tag{14}$$

By the condition (5), Eq. (14) and the Routh-Hurwitz theorem yield the necessary and sufficient condition for energetic stability, namely

$$a^2 < a_{\rm cr}^2 = \frac{\omega^2\gamma(\gamma+\nu)[4\omega^2 + \nu(2\gamma+\nu)]^2}{16\omega^2\gamma(\gamma+\nu) + 2q\nu[4\omega^2\nu + (2\gamma+\nu)^3]}. \tag{15}$$

We note that in the case of dichotomous noise this condition for stability is in accordance with the results of [13]. Henceforth in this section we shall assume that the condition (15) is fulfilled. Turning now to the Eq. (13), we consider quantity N_1 in more detail. It follows from Eqs. (A5) and (13) that the time-homogeneous part of the second moment $M_{2,1}^{(as)} = \langle X^2\rangle_{as}$ is given by

$$N_1 = \frac{1}{S_2}(S_1 + 2D(\nu+\gamma)\{[4\omega^2 + \nu(\nu+2\gamma)]^2 - 16a^2(1-2q)\}), \tag{16}$$

where

$$\begin{aligned}S_1 = A_0((2\gamma+\nu)\{&8A_{11} + 4(2\gamma+\nu)A_9 - [4\omega^2 + \nu(2\gamma+\nu)]\\ &\times[2A_7 + (2\gamma+\nu)A_5]\} + (\gamma+\nu)(\gamma A_1 + A_3)\\ &\times\{[4\omega^2 + \nu(2\gamma+\nu)]^2 - 16a^2\} + 8qa^2\nu(2A_3 - \nu A_1))\end{aligned} \tag{17}$$

and

$$S_2 = 2\omega^2\gamma(\gamma+\nu)[4\omega^2 + \nu(2\gamma+\nu)]^2\left[1 - \left(\frac{a}{a_{cr}}\right)^2\right]. \tag{18}$$

Particularly, the time-homogeneous part of the variance of the oscillator displacement X can be expressed as

$$\sigma^2(X) = \frac{\Omega}{2\pi}\int_0^{2\pi/\Omega}(\langle X^2\rangle_{as} - \langle X\rangle_{as}^2)dt = N_1 - \frac{A^2}{2}. \tag{19}$$

Evidently, if the noise amplitude a tends to the critical value $a_{\rm cr}$, the second moment $\langle X^2\rangle_{as}$ diverges.

The two-time correlation function $\langle X(t+\tau)X(t)\rangle_{as} - \langle X(t+\tau)\rangle_{as}\langle X(t)\rangle_{as}$ in the limit $t\to\infty$ depends on both times t and τ and becomes a periodic function of t with the period of the external driving, $T = 2\pi/\Omega$. Thus, as in [23], we define the one-time correlation function $K_1(\tau)$ as the average of the two-time correlation function over a period of the external driving, i.e.,

$$K_1(\tau) = \frac{1}{T}\int_0^T dt[\langle X(t+\tau)X(t)\rangle_{as} - \langle X(t)\rangle_{as}\langle X(t+\tau)\rangle_{as}]. \tag{20}$$

Using Eqs. (1), (6), and (9) we obtain

$$K_1(\tau) = \sum_{j=1}^{6} C_j e^{\rho_j\tau} + e^{-\nu\tau}[B_1\sin(\Omega\tau) + B_2\cos(\Omega\tau)], \tag{21}$$

where ρ_j are the roots of Eq. (8) and the constants C_j are determined by the nonhomogeneous system of six linear algebraic equations,

$$\sum_{j=1}^{6} L_{i,j}C_j = N_i - B_{2i} - \frac{1}{2}(A_1A_{2i-1} + A_2A_{2i}), \tag{22}$$

where $i=1,\ldots,6$, the coefficients $L_{i,j}$ are the same as in Eq. (A2), and the quantities $N_i, i=2,\ldots,6$, and $B_1, B_{2i}, i=1,\ldots,6$ are given by Eqs. (A6)–(A8) in the Appendix. Thus the one-time correlator

$$K(\tau) = \frac{1}{T}\int_0^T dt\langle X(t+\tau)X(t)\rangle_{as} \tag{23}$$

can be written exactly as the sum of two contributions,

$$K(\tau) = K_1(\tau) + K_2(\tau), \quad K_2(\tau) = \frac{A^2}{2}\cos(\Omega\tau), \tag{24}$$

i.e., the coherent part $K_2(\tau)$, which is periodic in τ with the period T, and the incoherent part $K_1(\tau)$, which decays to zero for large values of τ. Note that the real parts of ρ_j are negative. According to [23], the output SNR (R_{out}) at the forcing frequency Ω is defined in terms of the Fourier cosine transform of the coherent and incoherent parts of $K(\tau)$. Namely,

$$R_{\text{out}} = \frac{\Gamma_2}{\Gamma_1}, \tag{25}$$

where

$$\Gamma_2 = \frac{2}{T}\int_0^T d\tau K_2(\tau)\cos(\Omega\tau) = \frac{A^2}{2} \tag{26}$$

and

$$\Gamma_1 = \frac{2}{\pi}\int_0^\infty d\tau K_1(\tau)\cos(\Omega\tau)$$
$$= \frac{2}{\pi}\left(\frac{1}{\nu(\nu^2+4\Omega^2)}[\Omega\nu B_1 + (\nu^2+2\Omega^2)B_2]\right.$$
$$\left. - \sum_{j=1}^{6} C_j \frac{\rho_j}{\Omega^2+\rho_j^2}\right). \tag{27}$$

The SNR for an input signal $A_0\sin(\Omega t)+\xi(t)$ is given by

$$R_{\text{inp}} = \frac{A_0^2\pi}{4D}. \tag{28}$$

The SR gain Q is defined as the ratio of the output SNR to the input SNR, i.e.,

$$Q = \frac{R_{\text{out}}}{R_{\text{inp}}} = \frac{2DA^2}{\pi\Gamma_1 A_0^2}. \tag{29}$$

It is worth pointing out that the SR gain cannot exceed unity because of the linearity of the dynamical system (1), and it increases monotonically as D increases.

III. RESULTS

A. Energetic instability

Our next task is to find the boundaries of the region of energetic instability in the parameter space (ν,γ). The typical forms of the graph $a_{\text{cr}}^2(\nu)$ are represented in Fig. 1. From Eq. (15) one can discern two cases. First, if the damping is sufficiently strong, $\gamma > \gamma^*$, then the function $a_{\text{cr}}^2(\nu)$ increases monotonically from the value ω^4 to infinity as the switching rate ν increases [see curve (1) in Fig. 1]. Thus, by the condition (5) the system is stable, i.e., no energetic instability can occur. The critical damping parameter γ^* is given by the system of algebraic equations,

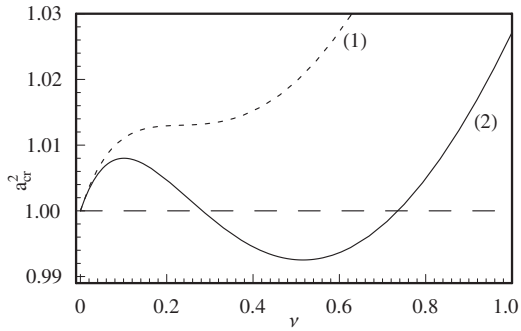

FIG. 1. Dependence of the critical noise amplitude a_{cr}^2 on the noise switching rate ν, obtained from Eq. (15). The parameter values: $\omega=1$, $q=0.35$. The dashed curve (1) and the solid curve (2) correspond to the values of the damping parameter $\gamma=0.33$ and $\gamma=0.3$, respectively. Note the nonmonotonous dependence of a_{cr}^2 on ν for $\gamma=0.3$.

$$\frac{d}{d\nu}a_{\text{cr}}^2(\nu) = 0, \quad \frac{d^2}{d\nu^2}a_{\text{cr}}^2(\nu) = 0, \tag{30}$$

where $a_{\text{cr}}^2(\nu)$ is given by Eq. (15). For example, in the case of dichotomous noise, $q=1/2$, the critical parameter $(\gamma^*)^2 = (3\sqrt{3}-5)\omega^2$. Second, in the case of $\gamma < \gamma^*$, Eq. (15) demonstrates that the functional dependence of a_{cr}^2 on the noise correlation time $\tau_c = 1/\nu$ exhibits a resonance form as τ_c is varied. For increasing values of ν, the critical noise amplitude a_{cr} starts from the value ω^2, increasing to a local maximum $a_{\text{cr max}}$, next it decreases, attaining a local minimum $a_{\text{cr min}}$, and then a_{cr} tends to infinity as $\nu\to\infty$ [curve (2) in Fig. 1]. Relying on Fig. 1 and Eqs. (5) and (15) one can find the necessary and sufficient conditions for the emergence of energetic instability (and reentrant transition) due to noise correlation time variations. Namely, energetic instability appears for the parameter values

$$\gamma < \gamma^*, \quad a_{\text{cr}}^2 < \omega^4, \quad a_{\text{cr min}}^2 < a^2 < \omega^4, \tag{31}$$

where $a_{\text{cr min}}^2$ corresponds to the local minimum of the function $a_{\text{cr}}^2(\nu)$. This case is characterized by the following scenario: For small values of the switching rate, $\nu < \nu_1$, where $a < a_{\text{cr}}(\nu)$, the system is stable. At $\nu=\nu_1$, i.e., $a=a_{\text{cr}}(\nu_1)$, the system becomes unstable. In the interval $\nu_1 < \nu < \nu_2$ of the switching rate there appears an instability, where the second moments of the oscillator displacements diverge. At $\nu=\nu_2$, where $a=a_{\text{cr}}(\nu_2)$, the energetic instability disappears and the system approaches the stable regime, thus making a reentrant transition. In Fig. 2 the scenario described above is illustrated for the damping parameter $\gamma=0.01$. Now, we will briefly consider the necessary condition for instability, $a_{\text{cr}}^2 < \omega^4$.

Figure 3 shows a phase diagram in the ν-γ plane at several values of q. The shaded region in the figure corresponds to those values of the parameters ν and γ at which energetic instability is possible. As the damping parameter γ increases the region of instability narrows down and disappears at the critical value of the damping parameter $\gamma_{\text{cr}}(q)$. Hence, there is an upper limit $\gamma_{\text{cr}}(q)$ for the damping parameter at greater values of which the instability cannot occur. The boundary of

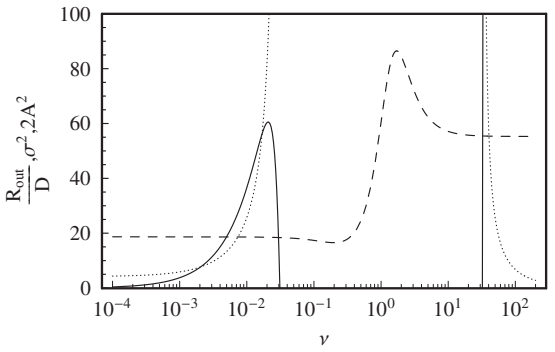

FIG. 2. Dependence of several SR characteristics: the output SNR (R_{out}), the variance (σ^2), and the SPA (A^2) computed from Eqs. (11), (19), and (25) with $A_0=\omega=1$, $\gamma=0.01$, $q=0.2$, $\Omega=0.9$, $a=0.9$, and $D=0.001$, on the noise switching rate ν. Solid line, R_{out}/D vs ν; dotted line, σ^2 vs ν; dashed line, $2A^2$ vs ν. In the interval $\nu \in (0.031, 32.9)$, the phenomenon of energetic instability occurs. Note the relatively rapid increase of SNR at $\nu \approx 32.9$.

the region of the instability phase and the critical parameter $\gamma_{cr}(q)$ are given by the fourth-order polynomial equation

$$[\nu(\nu+2\gamma)+4\omega^2][\nu\omega^2-\gamma(\nu+\gamma)(\nu+2\gamma)] = (1-2q)\omega^2[4\omega^2\nu+(\nu+2\gamma)^3]. \tag{32}$$

In the case of dichotomous noise, $q=1/2$, Eq. (32) reduces to a second-order equation and the boundary of the instability $\nu_{\pm}(\gamma)$ reads as

$$\nu_{\pm}(\gamma)=\frac{1}{2\gamma}(\omega^2-3\gamma^2 \pm \sqrt{\omega^4+\gamma^4-6\omega^2\gamma^2}). \tag{33}$$

Thus, in this case $\gamma_{cr}(\frac{1}{2})=\omega(\sqrt{2}-1)$. The tendency apparent in Fig. 3, viz. a decrease of γ_{cr} as the flatness parameter $\kappa=\frac{1}{2q}$ of the noise Z increases is a general feature of $\gamma_{cr}(q)$. Thus, in some parameter regimes energetic instability is possible, only if $\gamma<\omega(\sqrt{2}-1)$.

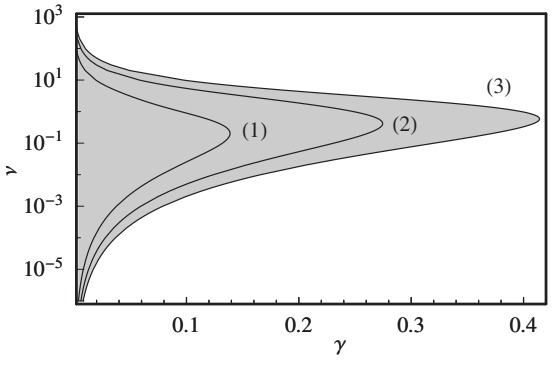

FIG. 3. A plot of the phase diagram in the ν-γ plane at $\omega=1$. The shaded domain in the figure corresponds to the region where noise-induced energetic instability is possible. The lines depict the borders of the energetic instability regions for several values of the noise parameter q, [see Eq. (32)]. The curves (1), (2), and (3) correspond to the values of the parameter $q=0.1$, $q=0.3$, and $q=0.5$, respectively.

Another important critical parameter is $a_{cr\ min}$, because of the conditions (31) for the occurrence of energetic instability. It follows from Eq. (15) that a_{cr}^2 decreases monotonically as the noise parameter q increases or as the damping coefficient decreases. The functional dependence of a_{cr} on the noise switching rate ν is more complicated, exhibiting several extrema (see Fig. 1). To get more information, we shall study it in the asymptotic limit of low damping. In general, the parameter $a_{cr\ min}$ can be found by numerical calculations from Eq. (15). In the low-damping limit, we allow γ to become small $\gamma \ll \gamma_{cr}$ and use γ as a perturbation parameter. In this case the critical parameter $a_{cr\ min}$, and the corresponding switching rate ν_m can be given as

$$a_{cr\ min}^2 \approx \frac{2\gamma\omega^3}{q}, \quad \nu_m \approx 2\omega - \frac{(2-q)\gamma}{q}. \tag{34}$$

The interesting feature of the result (34) is that Eq. (34) establishes a quantitative connection between stochastic oscillator instability and the parametric instability of a deterministic oscillator. Note that one of the trademarks of parametric resonance of the deterministic harmonic oscillator with a periodic perturbed frequency ω is that the most pronounced instability is induced by a superharmonic perturbation with the frequency $\omega_p \approx 2\omega$ [14]. Thus, the minimal value of the noise amplitude at which the instability of the oscillator develops corresponds to the noise switching rate which coincides with the leading frequency of the parametric resonance for a deterministic oscillator.

B. Response to noise amplitude

Next we consider the dependence of several SR characteristics on the noise amplitude a. In Fig. 4 we depict, on three panels, the behavior of A^2, σ^2, and the SR gain Q for various values of the temperature D. In the case considered, the critical noise amplitude ($a_{cr} \approx 0.995$) is very close to the maximal value of the noise amplitude, $a=1$. Here we emphasize that for all figures throughout this work we use a dimensionless formulation of the dynamics with $\omega=1$ and $A_0=1$. All SR characteristics exhibit a nonmonotonic dependence on the noise amplitude, i.e., a typical SR phenomenon continues to increase a. Clearly, additive thermal noise does not affect the spectral amplification A^2, but the variance σ^2 increases rapidly as the temperature D increases. For the parameter regime $a \ll a_{cr}$, the main contribution of the temperature appears as an additive term D/γ in σ^2 [cf. Eqs. (16)–(19)]. The main effect of temperature on the SR gain Q is that the resonance maximum of Q increases monotonically up to 1 as D increases.

As shown in Fig. 4(a), the curve A^2 vs a first exhibits a maximum and then a minimum appears, that is to say, the SR exhibited first is followed by a suppression. Most important, we observe that the resonance of SPA occurs for the noise amplitude $a \approx |\Omega^2-\omega^2|$, thus the resonance of SPA corresponds to the resonance frequency of the deterministic system for the fixed colored noise state $z_3=-a$. A resonancelike peak of the variance σ^2 at $a \approx |\Omega^2-\omega^2|$ is also observed [Fig. 4(b)]. This behavior of the variance, i.e., a strong amplification of the variance at the resonance peak of SPA, is quite

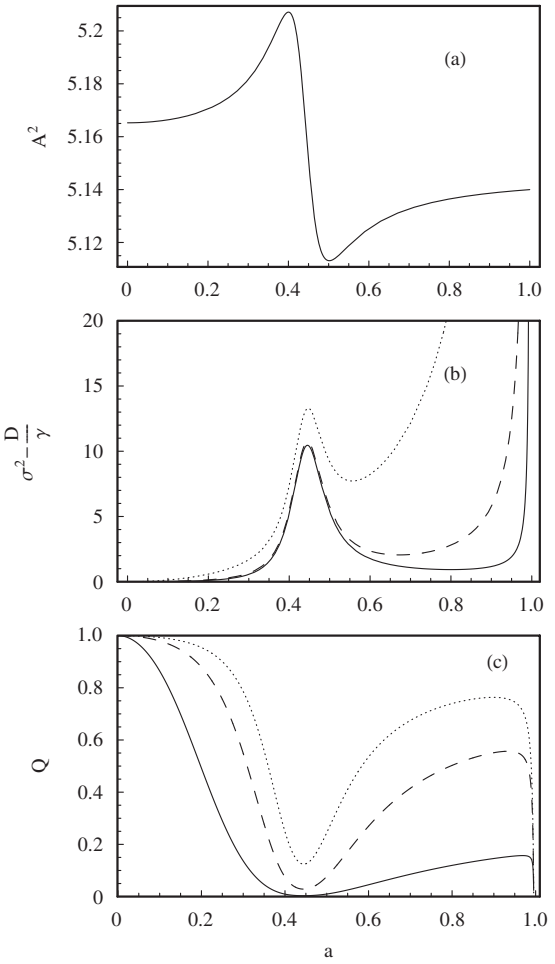

FIG. 4. SR characteristics [(a) the SPA (A^2), (b) the variance (σ^2), and (c) the SR gain (Q)] versus the noise amplitude a at several temperatures: $D_1=0.01$ (solid line), $D_2=0.1$ (dashed line), $D_3=1$ (dotted line) [Eqs. (11), (19), and (29)]. Parameter values: $\gamma=0.001$, $\nu=0.02$, $q=0.001$, $\Omega=1.2$, $\omega=A_0=1$. Note that the critical noise amplitude $a_{cr}\approx 0.9954$.

robust and occurs within a broad range of system parameters. With increasing the noise amplitude, one observes another region at the critical noise amplitude ($a\approx a_{cr}$), where the enhancement of the variance vs a is extremely rapid. Particularly, σ^2 increases unrestrictedly as energetic instability appears. Taking into account the behavior of σ^2, the highly nonlinear dependence of the SR gain Q on the amplitude a is not surprising [Fig. 4(c)]. It is intuitively clear that as the variance σ^2, i.e., the initial value of the incoherent part of the correlation function increases, the noise output spectral density $\Gamma_1(\Omega)$ [see Eq. (27)] increases as well. So the appearance of the resonance peak in the Q values is due to a very strong suppression of the SR gain by variance amplifications. Hence, the key factors for the appearance of SR in Q (as well as in R_{out}) are the occurrence of energetic instability and the resonance of SPA at some values of the noise amplitude a.

An interesting peculiarity of Fig. 4(a) is the rapid decrease of the SPA from the maximum to the minimum as a increases. It is noteworthy that in the case of dichotomous noise such an effect is absent. The effect is very pronounced at low values of the switching rate ν and a low damping γ

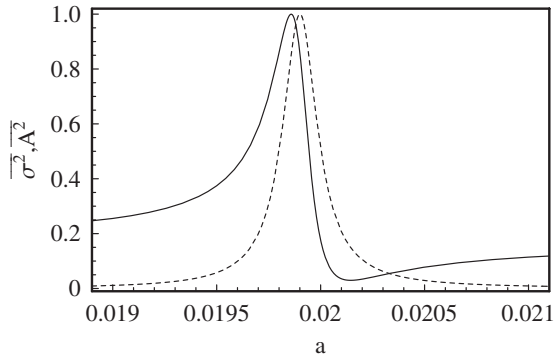

FIG. 5. A plot of the dependence of the SPA (A^2) and the variance (σ^2) on the noise amplitude a in a region of hypersensitive response [Eqs. (11) and (19)]. System parameters values: $\gamma=10^{-4}$, $\nu=10^{-6}$, $q=10^{-2}$, $\Omega=0.99$, $D=0$, and $A_0=\omega=1$. The values of A^2 and σ^2 at the local maximum are $A_m^2=14\,333$, $\sigma_m^2=495\,296$. The solid line and dotted line correspond to $\overline{A^2}\equiv A^2/A_m^2$ and $\overline{\sigma^2}\equiv\sigma^2/\sigma_m^2$, respectively.

(see Fig. 5). To throw some light on the physics of the abovementioned new effect, we shall now briefly consider the behavior of the SR characteristics A^2 and σ^2 in the parameter regime

$$\nu \ll \gamma \ll q|\omega^2-\Omega^2| \ll 1, \quad q \ll 1. \tag{35}$$

In this case, from Eqs. (A4) and (11) it follows that the SPA reaches the maximum $A_{max}^2\approx A_0^2q^2/(\Omega^2\gamma^2)$ at

$$a=a_{max}\approx|\Omega^2-\omega^2|$$

and the minimum $A_{min}^2\approx A_0^2\Omega^2\gamma^2/[q^2(\Omega^2-\omega^2)^4]$ at

$$a=a_{min}\approx\frac{|\Omega^2-\omega^2|}{\sqrt{1-2q}}.$$

For sufficiently strong inequalities (35), A_{min}^2 tends to zero and A_{max}^2 grows up to very large values. Thus in the case considered the SPA is extremely sensitive to a small variation of a: $\Delta a=a_{min}-a_{max}\approx q|\Omega^2-\omega^2|$. Note that this small interval of the noise amplitude, $a\in[|\Omega^2-\omega^2|,(1+q)|\Omega^2-\omega^2|]$, also contains a very narrow and high SR peak of the variance with the maximal value $\sigma_{max}^2\approx A_0^2q/(2\Omega^2\gamma^2)$. The above formulas for A_{max}^2 and σ_{max}^2 indicate that the main mechanism for the formation of SR in the SPA and σ^2 is the conventional amplitude-resonance generated by an external periodic forcing with the frequency $\Omega=\sqrt{\omega^2\pm a}$. More precisely, consider an ensemble of realizations of the stochastic oscillator for each of which a particular sequence of switching times, between the states of the nonequilibrium noise $Z(t)$, is chosen from the distribution of switching times. For a given time moment t the relative amount of realizations with the noise state $z_3=-a$ is q. As the switching rate ν and the damping coefficient γ are small (the noise correlation time is long) there is, between two switchings of the noise $Z(t)$, enough time for a very strong amplification of the amplitude of $X(t)$, which happens in the noise state $z_3=-a$ due to the conventional resonance at $\Omega=\sqrt{\omega^2-a}$. Particularly, in the state $z_3=-a$ all these realizations are strongly synchronized because of the phase lag $\varphi=-\pi/2$ between the periodic driving force

and the periodic response of the system by resonance. Therefore, although the fraction of such realizations is low ($q \ll 1$), the contribution of these realizations still dominates by the formation of SR in the SPA because of high amplitudes and synchronization. As the noise amplitude increases, the drastic decrease of SPA and also the appearance of the resonant amplification of the variance (see Fig. 5) indicate a rapid desynchronization of the realizations of the stochastic oscillator. Note that the above scenario accords with calculations of the phase lag φ for the mean displacement of the oscillator [Eq. (12)]. For example, in the case of the system parameters used in Fig. 5 the result is as follows: As a is gradually increased from zero and swept through the resonant amplitude $a \approx 0.02$, φ first decreases very slowly and later quickly from zero, passes through $-\pi/2$ when $a \approx 0.02$, and quickly approaches zero when $a > 0.02$.

C. Response to noise correlation time

The qualitative behavior of the SR characteristics A^2, σ^2, and R_{out} versus the noise correlation time $\tau_c = 1/\nu$ is sensitive to values of other system parameters. In the case exposed in Fig. 2, for the variance σ^2 the SR phenomenon is absent, σ^2 increases monotonically to infinity as ν tends to ν_1, $a = a_{\text{cr}}(\nu_1)$, i.e., instability appears; next, if $\nu > \nu_2 > \nu_1$, $a = a_{\text{cr}}(\nu_2)$, σ^2 decreases monotonically from infinity to $D/\gamma = 0.1$. In contrast to the variance both the SPA (A^2) and the output SNR (R_{out}) vs ν exhibit SR. For the SPA the resonance maximum appears at the noise switching rate $\nu \approx 2$, which is in the region of energetic instability.

Here we remind the reader that SPA is determined with the first-order moment of the displacement of the oscillator and is therefore always stable. It is remarkable that the maximum of the SPA corresponds to the value of the noise switching rate at which the critical noise amplitude a_{cr} is minimal, i.e., the growth rate of displacement realizations is maximal. The explanation of this stability in terms of our parametric oscillator description is that in the averaging procedure, displacements that grow exponentially in the positive direction are canceled by others that grow exponentially in the negative direction [8]. For the output SNR one must discern two regions of ν values. If $\nu > \nu_2$ (the right stability region), the SNR grows monotonically from zero, while in the case of $\nu < \nu_1$ (the left stability region) SR appears. Note that the SNR always decreases to zero when the noise switching rate tends to zero or when energetic instability occurs ($\nu \to \nu_1$).

Though the behavior of SNR at ν_1 is a simple consequence of the circumstance that at the instability the noise output spectral density $\Gamma_1(\Omega)$ [Eq. (27)] tends to infinity, the behavior of SNR at $\nu \to 0$ is more supple. Namely, the limit $\nu \to 0$ for the noise output spectral density is not continuous: If $\nu > 0$, but very small, then the incoherent part $K_1(\tau)$ of the correlator (23) decreases very slowly as τ increases [see Eq. (21)]. Because of this, $\Gamma_1(\Omega)$ is very large and tends to infinity as $\nu \to 0$, while the SNR tends to zero; if $\nu = 0$, the term which is proportional to $\exp(-\nu\tau)$ in Eq. (21) is a periodic function and as such should be considered in the coherent part $K_2(\tau)$ of the correlator (23). In the last case ($\nu = 0$) the noise output spectral density is finite.

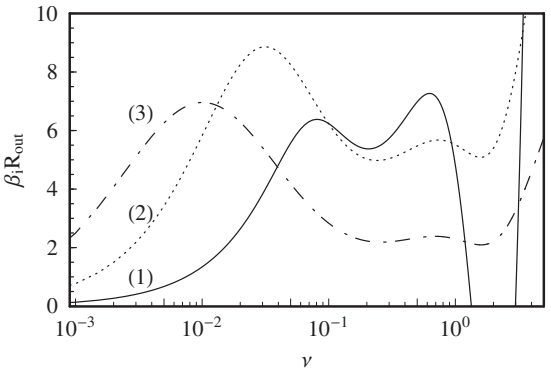

FIG. 6. SNR (R_{out}) versus the noise switching rate ν at $\omega = A_0 = 1$ for several parameter regimes [Eq. (25)]. Solid line, $\beta_1 = 1$, $\gamma = 7 \times 10^{-4}$, $D = 10^{-3}$, $q = 0.5$, $a = 0.055$, $\Omega = 0.8$; dotted line, $\beta_2 = 4$, $\gamma = 10^{-3}$, $D = 0.1$, $q = 0.41$, $a = 0.061$, $\Omega = 1.2$; dashed-dotted line, $\beta_3 = 12$, $\gamma = 10^{-3}$, $D = 1$, $q = 0.41$, $a = 0.061$, $\Omega = 1.2$. In the case of curve (1) (solid line) energetic instability occurs in the interval $\nu \in (1.338, 2.981)$.

As mentioned above, there are certain ranges of system parameters for which the behavior of SR characteristics can be qualitatively different. A plot (Fig. 6) of the output SNR vs the noise switching rate for different system parameters shows a double resonant peak structure with quite different heights of peaks. This double resonant structure can be interpreted as the splitting of the resonant peak considered by Fig. 2, which is due to the nonlinear influence of noise correlation time on the noise output spectral density. Note that the second minima of the curves (2) and (3) in Fig. 6 correspond to the noise switching rate $\nu \approx 2$ at which the critical noise amplitude is minimal, $a_{\text{cr min}} \approx 0.07$, and the variance σ^2 is maximal [see Fig. 7, curve (3)]. It is remarkable that for the parameter regimes considered by the curves (2) and (3) in Fig. 6 the variance exhibits a single-peak form of SR, as shown in Fig. 7 with curve (3). The SPA is, in this case, rather a decreasing function of ν, while the SR phenomenon is absent.

The phenomenon of multiresonance is not restricted to the output SNR. Figure 7 depicts double-peak SR for the vari-

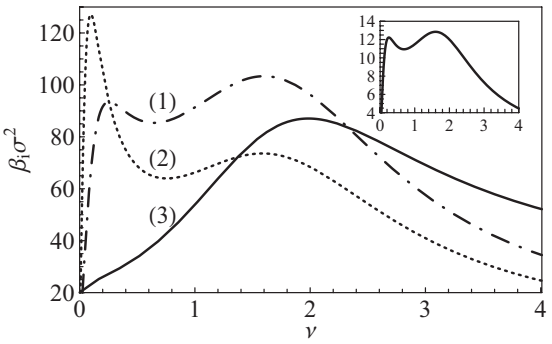

FIG. 7. Variance of the output signal (σ^2) versus the noise switching rate ν for different values of the external forcing frequency Ω and temperature D [Eq. (19)]. The system parameter values: $A_0 = \omega = 1$, $\gamma = 10^{-3}$, $q = 0.41$, $a = 0.061$. Dashed-dotted line, $\beta_1 = 5$, $\Omega = 0.8$, $D = 0$; dotted line, $\beta_2 = 1$, $\Omega = 0.9$, $D = 0$; solid line, $\beta_3 = 0.2$, $\Omega = 1.2$, $D = 0.1$. The inset depicts σ^2 vs ν in the parameter regime, $\Omega = 1.2$, $D = 0$.

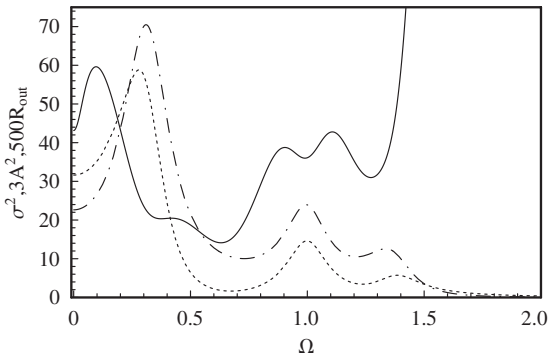

FIG. 8. SR characteristics [the SPA (A^2), variance (σ^2), and SNR (R_{out})] as functions of the frequency Ω of an external field [Eqs. (11), (19), and (25)]. The parameter values: $A_0=\omega=1$, $\gamma=0.1$, $a=0.9$, $\nu=0.1$, $q=0.3$, $D=0$. Solid line, $500R_{out}$ vs Ω; dotted line, $3A^2$ vs Ω; dashed-dotted line, σ^2 vs Ω.

ance σ^2 vs ν for different values of the driving frequency Ω. Although, in the case of $a<a_{cr\,min}$ the position of the second peak is nearly independent of Ω, it is determined by the value of ν at the minimum of $a_{cr}(\nu)$: The first peak of the variance quite strongly depends on Ω as both its magnitude and its position change. If $\Omega<1$, then with an increase of Ω the magnitude of the first peak of σ^2 increases more rapidly than the magnitude of the second peak, while its position shifts towards smaller values of the noise switching rate. In the case of $\Omega>1$, the second peak is more pronounced than the first. Particularly for variance the phenomenon of multiresonance is sensitive to input thermal noise. As the temperature D increases from zero the double-peak structure of SR disappears and the SR is characterized by a single-peak form [cf. the inset and curve (3) in Fig. 7].

D. Bona fide resonance

The dependence of the SR characteristics A^2, σ^2, R_{out}, and Q on the frequency Ω of the input signal is shown in Figs. 8 and 9 for different parameter regimes. These graphs show a typical resonance, with nonmonotonic behavior for the frequencies Ω close to several resonance frequencies, which is a bona fide resonance phenomenon. For zero temperature, but intermediate values of other parameters (Fig. 8), the positions of the resonance peaks for SPA and variance reproduce quite exactly the three-level structure of the multiplicative noise $Z(t)$. These three resonance peaks occur at the frequencies $\Omega_1\approx\sqrt{\omega^2-a}$, $\Omega_2\approx\omega$, and $\Omega_3\approx\sqrt{\omega^2+a}$, which correspond to the noise states $z_1=-a$, $z_2=0$, and $z_3=a$, respectively. The monotonic decrease of the height of the resonance peaks mimics the decrease of the resonant amplitude of the periodically forced deterministic oscillator as the resonant frequency increases. For the output SNR the picture of the graph is more complicated, exhibiting eight local extremums. Compared to the SNR and variance, it is seen that the three minima of R_{out} correspond to the three maxima of σ^2. The second minimum and maxima form due to different nonlinear behaviors of the characteristics $\Gamma_2(\Omega)$ and $\Gamma_1(\Omega)$ of the coherent and incoherent parts of the correlator $K(\tau)$ [Eqs. (25)–(27)].

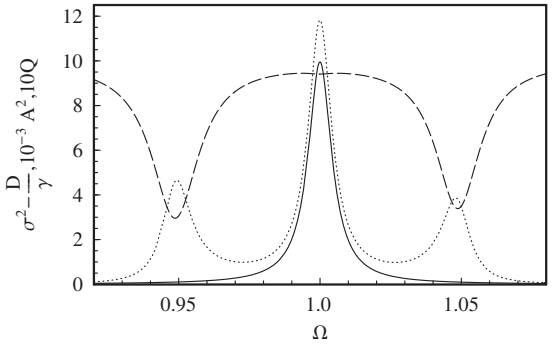

FIG. 9. Dependence of the SR characteristics [SPA (A^2), the variance (σ^2), and the SR gain (Q)] computed from Eqs. (11), (19), and (29) for $A_0=\omega=1$, $\gamma=0.01$, $\nu=0.001$, $a=0.1$, $q=0.001$, $D=10$, on the frequency Ω. Dashed line, $10Q$ vs Ω; dotted line, $\sigma^2-(D/\gamma)$ vs Ω; solid line, $10^{-3}A^2$ vs Ω.

A new interesting phenomenon for the SR gain Q occurs at very small intensities of the multiplicative noise $Z(t)$ and at relatively high values of thermal noise. Figure 9 shows the dependence of A^2, σ^2, and Q on the frequency Ω at the following parameter values: $\gamma=0.01$, $\nu=0.001$, $a=0.1$, $q=0.001$, and $D=10$. Since the probability q for jumps to the states $z_1=a$ and $z_3=-a$ is very small, the secondary resonance peaks of the SPA are absent and the peaks of the variance are small. Actually, in the case of the system parameters applied in Fig. 9 the deviation of the values of σ^2, at the secondary peaks from the asymptotic value D/γ is less than 0.5%. However, quite surprisingly the SR gain Q shows two sharp (and strong) minima at supplementary resonant frequencies, $\Omega_1\approx\sqrt{\omega^2-a}$ and $\Omega_2\approx\sqrt{\omega^2+a}$. Thus in some cases, the investigation of the dependence of SR gain or of the output SNR versus the input signal frequency can yield important information about the structure of a multiplicative noise in oscillator devices, even if the intensity of the noise is very small. Finally, it is notable that in the case of dichotomous noise ($q=1/2$) such an effect is absent.

IV. CONCLUSIONS

In this work, we have analyzed the phenomena of SR and stochastic parametric resonance within the context of a noisy, harmonic oscillator with a fluctuating frequency driven by sinusoidal forcing and by an additive thermal noise. The frequency fluctuations are modeled as a colored three-level Markovian noise. The Shapiro-Loginov formula [21] allows us to find a closed system of equations for the first-order and second-order cumulants and the exact expressions for the long-time behavior of several SR characteristics, such as SPA, variance, SNR, and SR gain. A major virtue of the investigated model is that an interplay of three-level colored noise and the external periodic forcing in a noisy, harmonic oscillator can generate a rich variety of nonequilibrium cooperation effects.

One of our main results is that for a harmonic oscillator colored fluctuations of the frequency can cause correlation-time-induced transitions from energetic stability to instability as well as in the opposite direction. Furthermore, the transi-

tion is found to be reentrant, e.g., if the damping coefficient is lower than a certain threshold value, then the energetic instability appears above a critical value of the noise correlation time, but disappears again through a reentrant transition to the energetically stable state at a higher value of the noise correlation time.

As another main result we find the existence of a multiresonance behavior versus the noise correlation time of the variance and the SNR, and show that this phenomenon is significantly associated with the critical characteristics of stochastic parametric resonance. This finding complements the recent results reported in Refs. [15,16], where, in the case of dichotomous noise, mainly the behavior of the SPA of a noisy, harmonic oscillator is studied and a single-peaked SR versus correlation time is established.

Finally, it is remarkable that in the case of trichotomous noise there occur some phenomena, which are absent in the case of dichotomous noise, particularly: (i) In some parametric regions we have established the effect of a very sensitive response of SR characteristics to small variations of the noise amplitude (see Fig. 5), where, e.g., SPA displays a quick jump from a very high value to a low one as the noise amplitude increases but a little; (ii) surprisingly enough, at relatively high temperatures and a large flatness of the colored noise, the SR gain versus the forcing frequency shows two pronounced, sharp minima, whereas for the SPA and variance the counterparts of such extrema can hardly be recognized (see Fig. 9). Those features of the stochastic oscillator are mainly of theoretical interest so far, as possible applications are not clearly identifiable yet. However, the result suggests that investigation of the SR gain versus input signal frequency can reveal important information about the structure of multiplicative noise in oscillator-devices, even if the intensity of the noise is very low. It seems that this possibility is worth being addressed in detail in some future study. Furthermore, in the case of trichotomous noise the results indicate that SR phenomena are sensitive to noise flatness, which is defined as the ratio of the fourth moment to the square of the second moment of the noise process. Thus, it is important to investigate the influence of the flatness of fluctuations on the stochastic resonant phenomena in more detail.

ACKNOWLEDGMENTS

The research was partly supported by the Estonian Science Foundation Grant No. 7319 and the International Atomic Energy Agency Grant No. 14797.

APPENDIX: FORMULAS FOR THE COEFFICIENTS OF THE EXACT MOMENTS

Differential equations for the moments $M_{1,i}$

Using a procedure analogous to the one which is represented in [15], one obtains from Eqs. (1) and (6),

$$\dot{M}_{1,1} = M_{1,2},$$

$$\dot{M}_{1,2} = -\gamma M_{1,2} - \omega^2 M_{1,1} - M_{1,3} + A_0 \sin(\Omega t),$$

$$\dot{M}_{1,3} = M_{1,4} - \nu M_{1,3},$$

$$\dot{M}_{1,4} = -(\gamma + \nu) M_{1,4} - \omega^2 M_{1,3} - M_{1,5},$$

$$\dot{M}_{1,5} = M_{1,6} - \nu M_{1,5} + 2qa^2 \nu M_{1,1},$$

$$\dot{M}_{1,6} = -(\gamma + \nu) M_{1,6} - \omega^2 M_{1,5} - a^2 M_{1,3} + 2qa^2 \nu M_{1,2} + 2qa^2 A_0 \sin(\Omega t), \tag{A1}$$

where $\dot{M} \equiv \frac{dM}{dt}$.

Coefficients L_{ij} of Eq. (7)

The coefficients L_{ij}, $i,j=1,\ldots,6$, are given by formulas

$$L_{1,j} = 1, \quad L_{2,j} = \rho_j, \quad L_{3,j} = -[\omega^2 + \rho_j(\rho_j + \gamma)],$$

$$L_{4,j} = (\rho_j + \nu) L_{3,j}, \quad L_{5,j} = -L_{3,j}[(\rho_j + \nu)(\rho_j + \nu + \gamma) + \omega^2],$$

$$L_{6,j} = (\rho_j + \nu) L_{5,j} - 2qa^2 \nu, \tag{A2}$$

where the quantities ρ_j are the roots of the algebraic equation (8).

Coefficients of the first moments

Here we list the expressions of the coefficients A_k in Eq. (9),

$$A_1 = \frac{A_0[f_1 f_4 + f_3(f_2 + 2qa^2)]}{f_3^2 + f_4^2},$$

$$A_2 = \frac{A_0[f_1 f_3 - f_4(f_2 + 2qa^2)]}{f_3^2 + f_4^2},$$

$$A_3 = -\Omega A_2, \quad A_4 = \Omega A_1,$$

$$A_5 = A_0 + (\Omega^2 - \omega^2) A_1 + \Omega \gamma A_2,$$

$$A_6 = (\Omega^2 - \omega^2) A_2 - \Omega \gamma A_1,$$

$$A_7 = \nu A_0 + [\nu(\Omega^2 - \omega^2) + \gamma\Omega^2] A_1 + \Omega[\nu\gamma - (\Omega^2 - \omega^2)] A_2,$$

$$A_8 = \Omega A_0 + \Omega[(\Omega^2 - \omega^2) - \nu\gamma] A_1 + [\gamma\Omega^2 + \nu(\Omega^2 - \omega^2)] A_2,$$

$$A_9 = \Omega A_8 - \omega^2 A_5 - (\nu + \gamma) A_7,$$

$$A_{10} = -\Omega A_7 - \omega^2 A_6 - (\nu + \gamma) A_8,$$

$$A_{11} = \nu A_9 - \Omega A_{10} - 2qa^2 \nu A_1,$$

$$A_{12} = \Omega A_9 + \nu A_{10} - 2qa^2 \nu A_2 \tag{A3}$$

where the quantities f_i $(i=1,\ldots,4)$ are determined as follows:

$$f_1 = 2\Omega(\gamma + 2\nu)[\nu(\gamma + \nu) + \omega^2 - \Omega^2],$$

$$f_2 = [\nu(\gamma + \nu) + \omega^2 - \Omega^2]^2 - \Omega^2(\gamma + 2\nu)^2 - a^2,$$

$$f_3 = [f_2(\omega^2 - \Omega^2) - \Omega\gamma f_1] - 2qa^2\nu(\nu + \gamma),$$

$$f_4 = [\Omega\gamma f_2 + (\omega^2 - \Omega^2)f_1] - 4qa^2\nu\Omega. \tag{A4}$$

Differential equations for the moments $M_{2,i}$

From Eqs. (1) and (6) nine linear differential equations can be obtained for the moments $M_{2,i}$, $i=1,\ldots,9$,

$$\dot{M}_{2,1} = 2M_{2,2},$$

$$\dot{M}_{2,2} = M_{2,7} - \gamma M_{2,2} - \omega^2 M_{2,1} - M_{2,3} + A_0 M_{1,1}\sin(\Omega t),$$

$$\dot{M}_{2,7} = -2\gamma M_{2,7} - 2\omega^2 M_{2,2} - 2M_{2,4} + 2A_0 M_{1,2}\sin(\Omega t) + 2D,$$

$$\dot{M}_{2,3} = -\nu M_{2,3} + 2M_{2,4},$$

$$\dot{M}_{2,4} = M_{2,8} - (\gamma + \nu)M_{2,4} - \omega^2 M_{2,3} - M_{2,5} + A_0 M_{1,3}\sin(\Omega t),$$

$$\dot{M}_{2,8} = -(2\gamma + \nu)M_{2,8} - 2\omega^2 M_{2,4} - 2M_{2,6} + 2A_0 M_{1,4}\sin(\Omega t),$$

$$\dot{M}_{2,5} = -\nu M_{2,5} + 2M_{2,6} + 2qa^2\nu M_{2,1},$$

$$\dot{M}_{2,6} = M_{2,9} - (\gamma + \nu)M_{2,6} - \omega^2 M_{2,5} - a^2 M_{2,3} + 2qa^2\nu M_{2,2} + A_0 M_{1,5}\sin(\Omega t),$$

$$\dot{M}_{2,9} = -(2\gamma + \nu)M_{2,9} - 2\omega^2 M_{2,6} - 2a^2 M_{2,4} + 2qa^2\nu M_{2,7} + 2A_0 M_{1,6}\sin(\Omega t) + 4qa^2 D \tag{A5}$$

with $\dot{M} \equiv \frac{dM}{dt}$.

Coefficients of the second moments

The time-homogeneous parts N_i of the moments $M_{2,i}^{(as)}$, $i=2,\ldots,6$, in Eqs. (13) and (22) are given by

$$N_2 = 0,$$

$$N_3 = \frac{1}{\nu + 2\gamma}[-2\gamma\omega^2 N_1 + A_0(\gamma A_1 + A_3) + 2D],$$

$$N_4 = \frac{\nu}{2}N_3,$$

$$N_5 = -\frac{1}{2}\left(2\omega^2 + \frac{\nu}{2}(\nu + 2\gamma)\right)N_3 + \frac{1}{2(\nu + \gamma)} \times \left[2qa^2\nu N_1 + A_0\left(A_7 + \frac{1}{2}(\nu + 2\gamma)A_5\right)\right],$$

$$N_6 = \frac{\nu}{2}N_5 - qa^2\nu N_1, \tag{A6}$$

where N_1 is determined by Eq. (16).

The coefficients B_1 and B_{2i}, $i=1,\ldots,6$, in Eqs. (21) and (22) can be given as

$$B_1 = \frac{F_1 G_1 + F_2\Omega G_2}{G_1^2 + \Omega^2 G_2^2},$$

$$B_2 = \frac{F_2 G_1 - F_1\Omega G_2}{G_1^2 + \Omega^2 G_2^2},$$

$$B_4 = \Omega B_1 - \nu B_2,$$

$$B_6 = [(\Omega^2 - \omega^2) - \nu(\nu - \gamma)]B_2 + \Omega(2\nu - \gamma)B_1,$$

$$B_8 = \Omega\{[(\Omega^2 - \omega^2) - \nu(\nu - \gamma)]B_1 - \Omega(2\nu - \gamma)B_2\},$$

$$B_{10} = \Omega(\nu - \gamma)[2(\Omega^2 - \omega^2) + \nu\gamma]B_1 + \{(\Omega^2 - \omega^2)[(\Omega^2 - \omega^2) - \nu(\nu - \gamma)] + \gamma\Omega^2(2\nu - \gamma)\}B_2 + \frac{A_0 A_5}{2},$$

$$B_{12} = \Omega\{(\Omega^2 - \omega^2)[(\Omega^2 - \omega^2) - \nu(\nu - \gamma)] + \Omega^2\gamma(2\nu - \gamma)\}B_1 - \{\Omega^2(\nu - \gamma)[2(\Omega^2 - \omega^2) + \nu\gamma] + 2qa^2\nu\}B_2 + \frac{\Omega A_0 A_6}{2}, \tag{A7}$$

where

$$F_1 = \frac{A_0}{2}[2qa^2 A_2 - A_{10} - \gamma\Omega A_5 - (\Omega^2 - \omega^2)A_6],$$

$$F_2 = \frac{A_0}{2}[2qa^2 A_1 + \gamma\Omega A_6 - A_9 - (\Omega^2 - \omega^2)A_5],$$

$$G_1 = [(\Omega^2 - \omega^2)^2 + \Omega^2\gamma^2][(\Omega^2 - \omega^2) - \nu(\nu - \gamma)] + 2\Omega^2\gamma(\nu - \gamma)[2(\Omega^2 - \omega^2) + \gamma\nu] - a^2(\Omega^2 - \omega^2) + \nu(\nu - \gamma)a^2(1 - 2q),$$

$$G_2 = (2\nu - 3\gamma)[(\Omega^2 - \omega^2)^2 + \Omega^2\gamma^2] + 2\gamma(\nu - \gamma)[\nu(\Omega^2 - \omega^2) - 2\gamma\Omega^2] + a^2\gamma - 2\nu a^2(1 - 2q). \tag{A8}$$

[1] M. O. Magnasco, Phys. Rev. Lett. **71**, 1477 (1993); P. Reimann, Phys. Rep. **361**, 57 (2002); R. Tammelo, R. Mankin, and D. Martila, Phys. Rev. E **66**, 051101 (2002).

[2] J. García-Ojalvo and J. M. Sancho, *Noise in Spatially Extended Systems* (Springer-Verlag, New York, 1999).

[3] R. Mankin, A. Haljas, R. Tammelo, and D. Martila, Phys. Rev. E **68**, 011105 (2003); S. L. Ginzburg and M. A. Pustovoit, Phys. Lett. A **291**, 77 (2001); I. Bena, C. Van den Broeck, R. Kawai, and K. Lindenberg, Phys. Rev. E **66**, 045603(R) (2002).

[4] R. Benzi, A. Sutera, and A. Vulpiani, J. Phys. A **14**, L453 (1981); L. Gammaitoni, P. Hänggi, P. Jung, and F. Marchesoni, Rev. Mod. Phys. **70**, 223 (1998); B. McNamara and K. Wiesenfeld, Phys. Rev. A **39**, 4854 (1989); P. Jung and P. Hänggi, *ibid.* **44**, 8032 (1991); T. Wellens, V. Shatokhin, and A. Buchleitner, Rep. Prog. Phys. **67**, 45 (2004).

[5] R. Müller, K. Lippert, A. Kühnel, and U. Behn, Phys. Rev. E **56**, 2658 (1997); A. A. Zaikin, J. García-Ojalvo and L. Schimansky-Geier, *ibid.* **60**, R6275 (1999); S. Kim, S. H. Park, and C. S. Ryu, Phys. Rev. Lett. **78**, 1616 (1997); A. Sauga and R. Mankin, Phys. Rev. E **71**, 062103 (2005).

[6] C. C. Bloch, *Classical and Quantum Oscillator* (Wiley, New York, 1997).

[7] S. Chandrasekhar, Rev. Mod. Phys. **15**, 1 (1943).

[8] K. Lindenberg, V. Seshadri, and B. J. West, Phys. Rev. A **22**, 2171 (1980).

[9] J. I. Jiménez-Aquino, R. M. Velasco, and F. J. Uribe, Phys. Rev. E **77**, 051105 (2008); F. K. Abdullaev, S. A. Darmanyan, and M. R. Djumaev, Phys. Lett. A **141**, 423 (1989); P. S. Landa and A. A. Zaikin, Phys. Rev. E **54**, 3535 (1996); P. S. Landa, A. A. Zaikin, M. G. Rosenblum, and J. Kurths, *ibid.* **56**, 1465 (1997); C.-I. Um, K. H. Yeon, and T. F. George, Phys. Rep. **362**, 63 (2002).

[10] M. Tureli, *Theoretical Population Biology* (Academic, New York, 1977).

[11] N. G. van Kampen, *Stochastic Processes in Physics and Chemistry* (North-Holland, Amsterdam, 1981).

[12] V. I. Klyatskin, *Stochastic Equations Through the Eye of the Physicist: Basic Concepts, Exact Results and Asymptotic Approximations* (Elsevier, Amsterdam, 2005).

[13] R. C. Bourret, U. Frisch, and A. Pouquet, Physica (Utrecht) **65**, 303 (1973).

[14] I. Bena, C. Van den Broeck, R. Kawai, M. Copelli, and K. Lindenberg, Phys. Rev. E **65**, 036611 (2002).

[15] M. Gitterman, Phys. Rev. E **67**, 057103 (2003).

[16] M. Gitterman, Physica A **352**, 309 (2005).

[17] V. Berdichevsky and M. Gitterman, Phys. Rev. E **60**, 1494 (1999).

[18] L. Gammaitoni, F. Marchesoni, and S. Santucci, Phys. Rev. Lett. **74**, 1052 (1995); S. Jiang, F. Guo, Y. Zhou, and T. Gu, Physica A **375**, 483 (2007).

[19] R. Mankin, A. Ainsaar, and E. Reiter, Phys. Rev. E **60**, 1374 (1999); R. Mankin, A. Ainsaar, A. Haljas, and E. Reiter, *ibid.* **63**, 041110 (2001).

[20] C. R. Doering, W. Horsthemke, and J. Riordan, Phys. Rev. Lett. **72**, 2984 (1994).

[21] V. E. Shapiro and V. M. Loginov, Physica A **91**, 563 (1978).

[22] S. Roul, *Programming for Mathematicians* (Springer-Verlag, Berlin, 2000), Sec. 10.13, pp. 280–286.

[23] J. Casado-Pascual, J. Gómez-Ordóñez, M. Morillo, and P. Hänggi, Phys. Rev. E **68**, 061104 (2003).